

Growth of Cu₂S Ultrathin Nanowires in a Binary Surfactant Solvent

Zhaoping Liu,[†] Dan Xu,[†] Jianbo Liang,[†] Jianming Shen,[†] Shuyuan Zhang,^{†,‡} and Yitai Qian^{*,†,‡}

Structure Research Laboratory and Department of Chemistry, University of Science and Technology of China, Hefei, Anhui 230026, People's Republic of China

Received: January 19, 2005; In Final Form: March 5, 2005

We demonstrate a facile solution-phase method for the synthesis of single-crystal, high aspect ratio, and ultrathin nanowires of hexagonal-phase Cu₂S by thermal decomposition of CuS₂CNEt₂ in a mixed surfactant solvent of dodecanethiol and oleic acid at 160 °C. Cu₂S nanowires can be controllably synthesized with a diameter as thin as 1.7 nm and length up to tens of micrometers; they are usually aligned in the form of bundles with a thickness of hundreds of nanometers. Based on the experimental results, the formation mechanism of the ultrathin nanowires has been properly proposed. Some key synthetic parameters, which have a significant effect on the sizes and shapes of the products, have also been investigated in detail. UV–vis spectroscopy measurement reveals that the resultant ultrathin nanowires show a strong quantum size effect.

Introduction

In the past decade, one-dimensional (1D) nanoscale building blocks, such as nanowires, nanorods, and nanotubes, have attracted intensive interest due to their potential applications in nanodevices.¹ Many recent efforts have been focused on the development of new synthetic methodologies for fabricating inorganic nanowires with small diameters and high aspect ratio.² Nevertheless, methods for controlling the diameters of less than 10 nm and lengths of larger than 10 μm are still limited and represent an important challenge in nanowire synthesis. The relatively successful method for generating high aspect ratio and ultrathin nanowires is template direct synthesis by using the channels contained in mesoporous silica,^{2a} reverse micelles,^{2f} and so on. Recently, a solution-phase method using surfactants (such as long-chain amines, phosphine, phosphine acids, and carboxylic acids) as the reaction solvent has been developed for the synthesis of semiconductors and metal nanowires with diameters less than 10 nm.³ However, the lengths of most of the nanowires were generally limited to micrometer scale. Hence, it is necessary to explore the further use of this solution-phase method for the synthesis of high aspect ratio and ultrathin nanowires in the surfactant solvent.

Cu₂S (chalcocite) is an indirect semiconductor with a bulk band gap of 1.21 eV,⁴ and it has been extensively investigated and widely used as a component of solar cells.⁵ The availability of Cu₂S nanostructures with well-defined morphologies and dimensions should enable bringing new types of applications or enhancing the performance of currently existing photoelectric devices due to the quantum-size effects. Recently, Cu₂S nanostructures have attracted particular attention and various synthetic schemes have been developed for their synthesis. Cu₂S nanoparticles (or quantum dots) were successfully produced in microemulsions.⁶ Polycrystalline nanowires and nanotubes of Cu₂S were prepared by an organic amine assisted hydrothermal method.⁷ Single-crystalline nanowire arrays of monoclinic Cu₂S with 10–100 nm diameters were grown at room temperature

by flowing H₂S gas on a Cu substrate.⁸ As first reported by Korgel and co-workers,⁹ rodlike and disklike nanocrystals of hexagonal Cu₂S could be selectively synthesized by a solventless thermolysis of a copper thiolate precursor; thereafter, Wu et al. found that Cu₂S nanowire with diameters of 2–6 nm and lengths up to several micrometers could be generated by the use of a highly polymerized copper thiolate precursor.¹⁰ We have also reported the synthesis of monodispersed nanocrystals of hexagonal Cu₂S through a reaction between copper salt and thioacetamide by using dodecanethiol as the solvent.¹¹ As part of our continuing effort to synthesize various nanostructures in the surfactant solvent, here we report on the synthesis of high aspect ratio and ultrathin nanowires of hexagonal Cu₂S by thermal decomposition of CuS₂CNEt₂ in a binary surfactant solvent of dodecanethiol (DT, C₁₂H₂₅SH) and oleic acid (OA, C₁₇H₃₃COOH).

Experimental Section

Synthesis. All chemicals were of analytical grade and were purchased from Shanghai Chemical Reagents Company. In a typical procedure, 0.5 mmol of CuCl₂·2H₂O was added in 20 mL of a mixed solvent of DT and OA (1/3, v/v) at room temperature, followed by an addition of 0.5 mmol of sodium diethyl dithiocarbamate (NaS₂CNEt₂). Then a dark yellow colloidal solution was formed by magnetic stirring. To avoid the oxidation of solvent, the reaction mixture was sealed in a Teflon bottle and then heated at 160 °C for 12 h in an electric oven. After reaction, the bottle was cooled to room temperature. The resulting brown solid product was collected by centrifugation, washed with distilled water and absolute alcohol several times to remove the byproducts and the excess surfactants, and finally dried at room temperature.

Characterization. The X-ray diffraction (XRD) analysis was performed using a Philip X'Pert PRO SUPER γA rotation anode with Ni-filtered Cu Kα radiation (λ = 1.541 78 Å). The transmission electron microscopy (TEM) images and electronic diffraction (ED) patterns were captured on a Hitachi Model H-800 instrument at an acceleration voltage of 200 kV. High-resolution TEM (HRTEM) images and selected-area electron

* To whom correspondence should be addressed. Phone: +86-551-3603204. Fax: +86-551-3607402. E-mail: yitqian@ustc.edu.cn.

[†] Department of Chemistry.

[‡] Structure Research Laboratory.

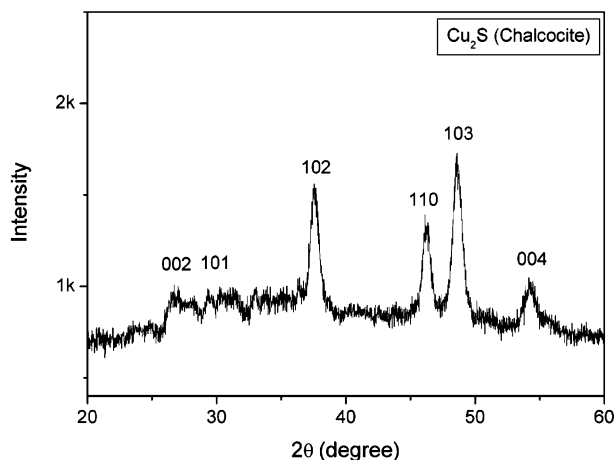


Figure 1. XRD pattern of the product.

diffraction (SAED) patterns were obtained on a JEOL-2010 transmission electron microscope at an acceleration voltage of 200 kV. Fourier transform infrared (FTIR) spectroscopy was performed with a Nicolet FTIR-170SX spectrometer in the range of 500–4000 cm^{-1} at room temperature, with the sample in a KBr disk. The absorption spectra were recorded on a UV–vis spectrophotometer (Shimadzu UV-240) in the wavelength range of 300–900 nm.

Results and Discussion

Structure and Morphology. Figure 1 shows a representative XRD pattern of the product; all the diffraction peaks can be well assigned to the hexagonal-phase Cu_2S (chalcocite) reported in the literature (JCPDS card, No. 84-206). The formation of hexagonal crystal structure of Cu_2S is reasonable since the present synthetic temperature (160 $^\circ\text{C}$) is higher than its phase transition temperature (105 $^\circ\text{C}$), at which Cu_2S undergoes a structural transition from monoclinic to hexagonal.¹² This result also indicates that the as-prepared Cu_2S still retains its hexagonal crystal structure at room temperature, in accord with previous reports about the Cu_2S nanostructure.⁹

A typical TEM image of the product is depicted in Figure 2a. This image reveals that the product consists of bundles of high aspect ratio and ultrathin nanowires. The inset in Figure 2a exhibits a typical nanowire bundle that has a length up to 50 μm . A high-magnification TEM image of a thin bundle of nanowires (see Figure 2b) clearly shows that the nanowires are rather uniform in diameter and are well aligned along their longitude direction, meaning that the nanowire bundles can be regarded as nanowire arrays in some local regions. The mean diameter of the individual nanowires constituting the bundles is estimated to be about 2.5 nm. From this image, the average interwire distance can also be measured to be about 1.3 nm.

The structural orientation of the as-prepared Cu_2S nanowires was investigated by analyzing a thin bundle with HRTEM and SAED. The SAED pattern inserted in Figure 2b, which was obtained by focusing the electronic beam on several aligned nanowires, indicates that the individual nanowires are of single crystals and can be indexed as hexagonal-phase Cu_2S , in accord with the XRD result. As can be seen, the $\pm(110)$ spots are highly elongated as a result of the locally orientationally ordered structure, and the elongated direction is perpendicular to the long axis of the nanowires, suggesting that these nanowires have a preferential growth direction of $[110]$. The HRTEM image shown in Figure 2c confirms that the bundle consists of single-

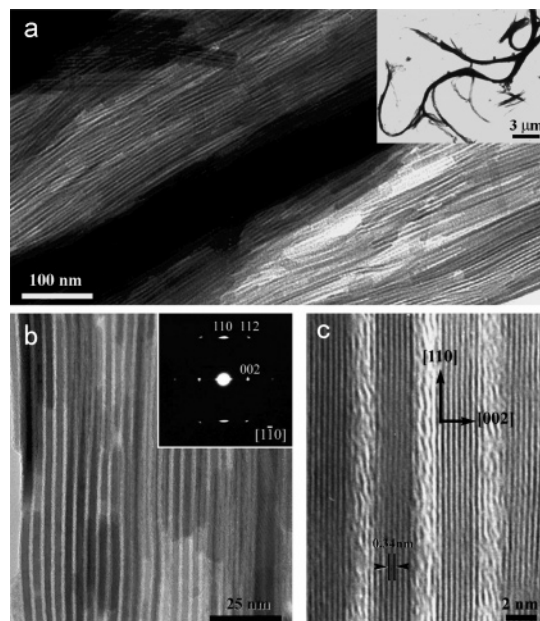
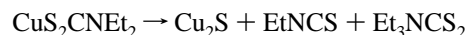


Figure 2. (a) Low-magnification, (b) high-magnification, and (c) high-resolution TEM images of Cu_2S nanowire bundles. The black zone in (a) represents a denser region of the nanowires. The inset in (a) exhibits a typical nanowire bundle. The inset in (b) shows the SAED pattern recorded from a thin region. The lattice spacing of 0.34 nm corresponds to the (002) crystal plane of hexagonal-phase Cu_2S .

crystal nanowires grown preferentially in the $[110]$ direction with the c -axis perpendicular to the long axis, agreeing well with the SAED result. From this image, it can be clearly seen that the diameters of individual nanowires are equal to just 7 or 8 times the (002) spacing of hexagonal-phase Cu_2S .

Growth Process and Possible Growth Mechanism. In our synthesis, a white slurry was formed first after the addition of $\text{CuCl}_2 \cdot 2\text{H}_2\text{O}$ into the mixed surfactant solvent, suggesting the reduction of Cu(II) to Cu(I) by $\text{C}_{12}\text{H}_{25}\text{SH}$. The further addition of $\text{NaS}_2\text{CNET}_2$ resulted in the formation of a molecular precursor, $\text{CuS}_2\text{CNET}_2$, as evidenced by an immediate dark yellow color change. For conveniently observing the changes that occurred during the reaction, the dark yellow slurry was heated alternatively in a flask. We noted that the slurry was changed to a clear dark yellow solution at about 110 $^\circ\text{C}$, indicating that $\text{CuS}_2\text{CNET}_2$ could be easily dissolved into the warm DT–OA solvent. Soon, a red brown turbidity appeared as the temperature was further elevated, suggesting the nucleation of Cu_2S had occurred. If no $\text{NaS}_2\text{CNET}_2$ was added, the hot solution was yellowish, and no precipitate could be produced even at a temperature as high as 180 $^\circ\text{C}$. This means that the manner of the Cu_2S formation in the present solution-phase method is very different from that in the solventless route previously reported by Korgel and Wu, in which they believed that Cu_2S was produced by thermolysis of Cu(I) thiolate precursor.^{9,10} On the basis of our real observation, it could be safely concluded that Cu_2S was generated by the thermal decomposition of $\text{CuS}_2\text{CNET}_2$. The involved chemical reaction may be expressed by the following formula that is analogous to the previous report about the thermal fragmentation of $\text{Zn(S}_2\text{CNET}_2)_2$:¹³



In a recent report,¹⁴ a similar precursor, $\text{Cu(S}_2\text{CNET}_2)_2$, was also used for the synthesis of $\text{Cu}_{1.8}$ (digenite) quantum dots; the decomposition reaction was performed in tri-*n*-octylphosphine oxide (TOPO) at 250 $^\circ\text{C}$.

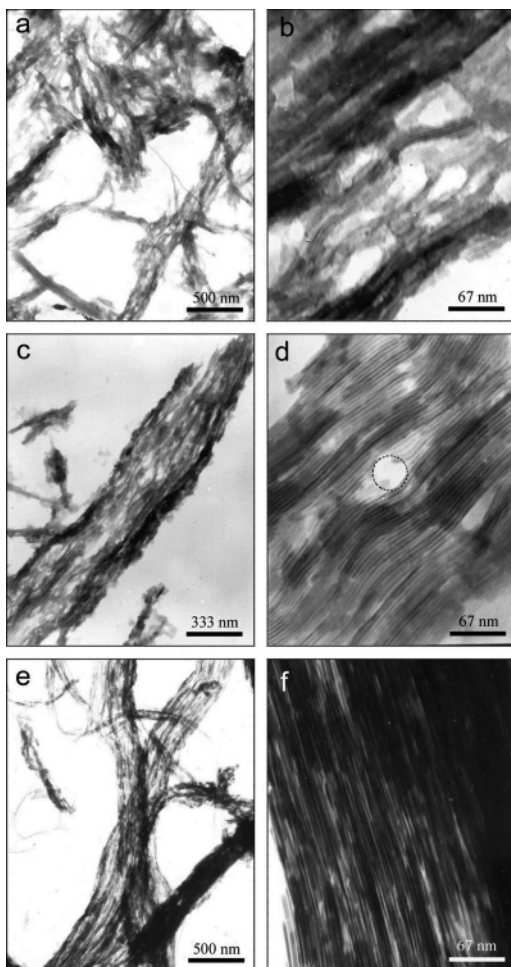


Figure 3. Low- and high-magnification TEM images of samples prepared at different reaction stages: (a, b) 2, (c, d) 5, and (e, f) 8 h. A typical vacancy in the nanowire bundles is labeled by the broken circle in panel d.

After continuously heating the reaction mixture for about 12 h, bunchy ultrathin nanowires were formed, as demonstrated by Figure 2. The growth process of these nanowire bundles was monitored by systematically investigating the samples obtained at various stages of the reaction using TEM. Figure 3 shows low- and high-magnification TEM images of the samples that were obtained after the reaction proceeded at 160 °C for 2, 5, and 8 h. These images clearly exhibit the evolution of Cu₂S nanowire bundles over the periods of time. As can be seen in Figure 3a,b, the product obtained after 2 h of treatment was thin, short, and to some extent amorphous nanowire bundles with total length ranging from tens of nanometers to micrometer scale; also there were many vacancies in the bundles. As the reaction proceeded for 5 h, the bundles were much thicker and longer than before (see Figure 3c,d). Their thickness reached 400 nm and their length was increased to several micrometers; most of the vacancies had closed by continuous nanowires. After 8 h, the length of the bundles had developed into tens of micrometers, and little vacancies could be observed (see Figure 3e,f). On the basis of the above results, it could be believed that the formation of nanowire bundles had followed a ripening process. It should be noted, however, that the diameters of the individual nanowires constituting the bundles were kept almost unchanged at about 2.5 nm during the entire growth process, suggesting that the lateral surfaces of the nanowire might be passivated completely by surfactant molecules.

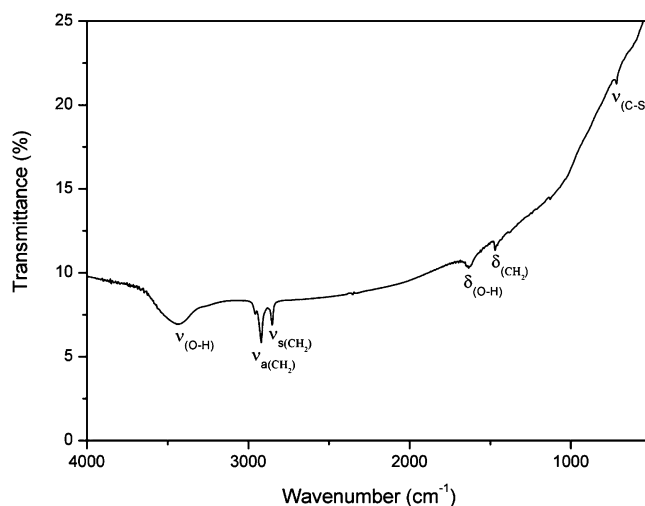


Figure 4. FTIR spectrum of as-prepared Cu₂S nanowire bundles.

As we know, the use of surfactants for controlling the shapes and sizes of nanocrystallites in the solution-phase synthesis has been extensively demonstrated in recent studies; it has been generally accepted that the surfactant molecules serve as capping ligands and are able to modulate the growth kinetics of the growing nanocrystallites by interacting with various crystallographic facets at different strengths.^{3,15} For instance, in Korgel's and Wu's reports about the synthesis of Cu₂S nanoplates, nanorods, and nanowires by the solventless method, it was found that, between the two surfactants (octanoate and DT) used, only octanoate served as the capping ligands that stabilized particle sizes and shapes and also controlled the anisotropic growth, whereas DT just provided a sulfur source for Cu₂S.^{9,10} In our synthesis, however, the mixture of the two surfactants, DT and OA, was employed as the solvent. As described above, we have confirmed that not DT but NaS₂CNEt₂ served as the sulfur source. Thus, what roles did DT and OA play additionally in terms of controlling the nanowire growth? Did both surfactants or only one of them serve as the capping ligands that induced and maintained 1D growth? For answering these important questions, some control experiments were carried out. When DT was used alone as the single solvent, the resulting product was platelike nanoparticles with sizes of 15–40 nm. In this case, no nanowires or nanorods could be obtained even if many other synthetic parameters were adjusted. This result was similar to that in our previous study, in which only Cu₂S nanoparticles were prepared by the reaction between Cu(I) thiolate and thioacetamide in pure DT solvent.¹¹ The use of OA alone, however, resulted in CuS flakes with sizes on the scale of micrometers. This was because the Cu(II) could not be reduced to Cu(I) in advance when DT was absent. Furthermore, when CuCl was used as the copper source instead of CuCl₂·2H₂O in this case, no nanowires were obtained yet. These results reveal that the use of either DT or OA alone does not induce the 1D growth of Cu₂S. We thus presume that a synergistic effect resulting from the combination of DT and OA may be responsible for the nanowire growth. However, which of them plays a major contribution to the controlling growth of nanowires? FTIR spectroscopy may be helpful to make this question clear. Figure 4 shows the FTIR spectrum of the as-prepared Cu₂S nanowires. The spectrum displays an absorption band at 720 cm⁻¹ characteristic of C–S stretching in the thiolate ions, but it does not exhibit bands at 1550 and 1411 cm⁻¹ characteristic of the –COO⁻ group. This feature suggests that DT may serve as the primary capping ligand for the nanowire

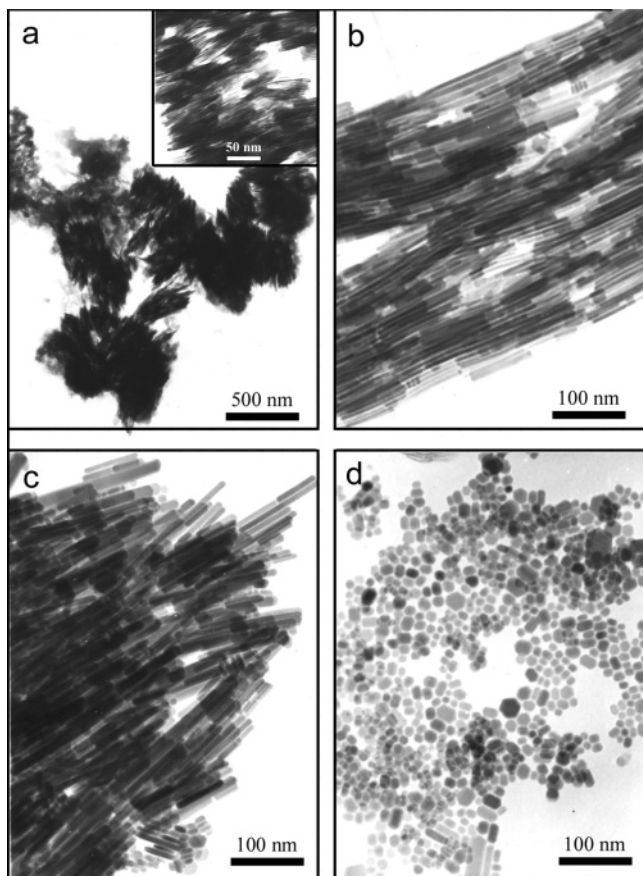


Figure 5. TEM images of samples prepared with various volume ratios of DT to OA: (a) 1/19, (b) 1/1, (c) 1.5/1, and (d) 3/1. The inset in (a) is an enlarged view of the thin and short nanorods.

growth by forming thiol-to-Cu(I) bonding on the surfaces of the growing Cu_2S nanocrystals and OA mainly acts as the solvent. This is reasonable since DT is a stronger ligand to the Cu_2S crystals in comparison with OA. It thus can be believed that the formation of Cu_2S ultrathin nanowires in our experiments may be attributed to the synergistic effect of the solvent OA and the adsorbent affinities of DT. To better understand the synergistic effect, we have investigated in detail the effect of the volume ratios of DT to OA on the sizes and shapes of the products. The experimental results revealed that the ultrathin nanowires were reproducibly produced only in an appropriate volume ratio of DT to OA, which was found to be in a range from 1/7 to 1/1.5. At a much small ratio of DT to OA (e.g., 1/19), the resulting product was short nanorods with diameters of about 2.5 nm and lengths of less than 100 nm, as shown in Figure 5a. On the other hand, when the ratio of DT to OA was increased to 1/1, the resulting nanowires had an increased diameter and a much decreased aspect ratio. Figure 5b is the TEM image of this sample, showing that the nanowires are about 5 nm thick and 100–200 nm long. At a higher ratio of 1.5/1, the product (see Figure 5c) was mainly composed of thicker nanorods with sizes of 10 nm \times 50–100 nm and included a small amount of 10–20 nm nanoparticles. Further increasing the ratio to 3/1, the product (see Figure 5d) was dominated by nanoparticles with sizes of 10–20 nm. These results indicate that only a relatively high proportion of OA can result in the formation of Cu_2S nanowires, further confirming that OA plays a major role of solvent and that combining it with DT has an interesting synergistic effect on 1D growth of Cu_2S nanowires.

Influence of the Relative Amounts of Copper and Sulfur Sources. In many previous studies about the chalcogenide

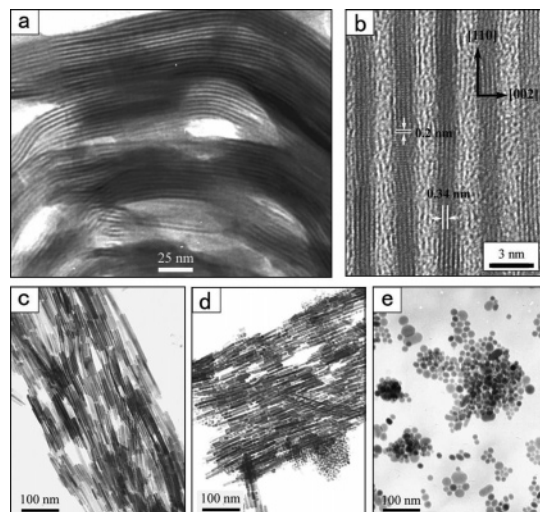


Figure 6. TEM images of samples prepared with various amounts of $\text{NaS}_2\text{CNET}_2$: (a) 1.0, (c) 0.6, (d) 0.68, and (e) 0.75 mmol. (b) HRTEM image of the same sample as shown in (a), in which the lattice spacings of 0.2 and 0.34 nm correspond to (110) and (002) crystal planes of hexagonal-phase Cu_2S , respectively.

nanostructures, it was found that the relative amounts (or the molar ratios) of metal salts and chalcogen source have a significant effect on the shapes and sizes of the resultant nanocrystals.^{15c,d} It has been generally believed that this result arose from the influence of the relative amounts of both reactants on the nucleation and growth of nanocrystals. In our synthesis, we also found that the shapes and sizes of the products were very sensitive to the relative amounts of copper and sulfur sources used. The diameter of nanowires decreased to a certain extent as solely the dose of $\text{CuCl}_2 \cdot 2\text{H}_2\text{O}$ was increased. For instance, using 1 mmol of $\text{CuCl}_2 \cdot 2\text{H}_2\text{O}$ and 0.5 mmol of $\text{NaS}_2\text{CNET}_2$, the resulting Cu_2S nanowires were only 1.7 nm in diameter, and they also assembled bundles with lengths up to 50 μm , but the bundles were much thinner than those prepared with 0.5 mmol of $\text{CuCl}_2 \cdot 2\text{H}_2\text{O}$ (see Figure 6a). The HRTEM image given in Figure 6b reveals that these nanowires are grown along the [110] direction and their diameters are equivalent to just 5 times the (002) spacing. On the other hand, with a relatively higher dose of $\text{NaS}_2\text{CNET}_2$, the produced nanowires had a increased diameter; further increasing its dose, the particle morphologies could be transformed from wires to rods and finally to particles. For example, with 0.6 mmol of $\text{NaS}_2\text{CNET}_2$, the product (see Figure 6c) consisted of much shorter nanowires (50–300 nm) with a diameter of about 4 nm; as the $\text{NaS}_2\text{CNET}_2$ dose was increased to 0.68 mmol, a mixture of nanorods (8 nm \times 50–200 nm) and nanoparticles (8 nm) was obtained (see Figure 6d); with a higher dose up to 0.75 mmol, only nanoparticles of 10–20 nm diameters were generated, as shown in Figure 6e.

Influence of the Reaction Temperature. Temperature was found to be another key factor that could affect the sizes and shapes of the products. Although a wide range of temperatures from 130 to 165 $^\circ\text{C}$ was found to be suitable for the high-yield synthesis of Cu_2S nanowires, a relatively lower temperature resulted in smaller and shorter nanowires bundles with poorer crystallinity. Parts a and b of Figure 7 exhibit the low- and high-magnification TEM images, respectively, of the samples prepared at 130 $^\circ\text{C}$. These images show that the diameters of nanowires were reduced to about 1.8 nm but most of the bundles were thin and short, suggesting that a relatively longer period of the ripening process was needed for the evolution of long nanowires. However, a overly high temperature was found to

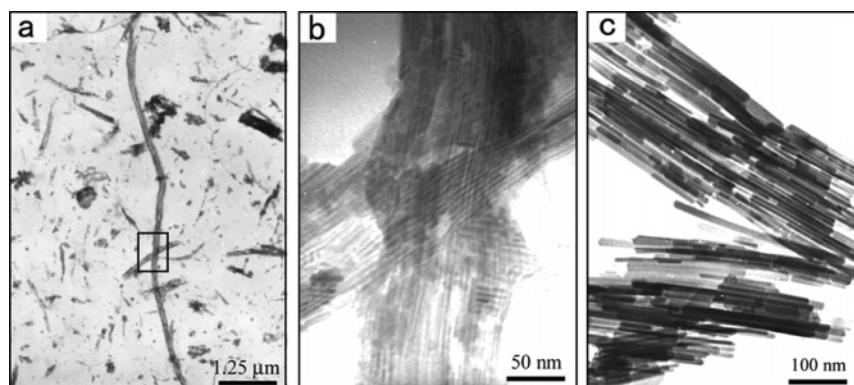


Figure 7. (a) TEM image of sample prepared at 130 °C. (b) Enlarged view of the boxed region in (a). (c) TEM image of sample prepared at 175 °C.

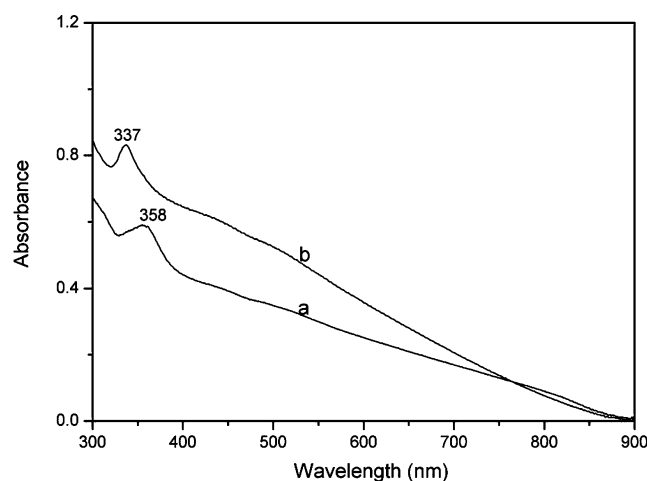


Figure 8. Room-temperature UV-vis absorption spectra of as-prepared Cu₂S ultrathin nanowires with respective average diameters of (a) 2.5 and (b) 1.7 nm.

result in much thicker nanowires (or nanorods), possibly due to a weakened adsorption effect between the capping ligands and the {002} planes of Cu₂S nanocrystallites. Figure 7c presents a TEM image of a sample prepared at 175 °C. It can be seen that the product consists of thick and short nanorods that are 5–15 nm thick and 50–300 nm long.

Optical Property. In a previous study,^{6a} Cu₂S nanoparticles prepared in microemulsions were reported to show a blue-shift peak (475 nm) in the UV-vis absorption spectrum compared to that of bulk phase (1022 nm),⁴ indicating the presence of the size quantization effect. Because the as-prepared Cu₂S ultrathin nanowires have a thickness as thin as <2.5 nm, a strong quantum size effect should be expected for them. Curves a and b of Figure 8 show the room-temperature UV-vis absorption spectra of the as-prepared Cu₂S nanowires with average diameters of 2.5 and 1.7 nm, respectively. A marked absorption peak appears at 358 and 337 nm for 2.5 and 1.7 nm diameter nanowires, respectively; there are long tails in the curves, which may be attributed to the very high aspect ratio of the as-prepared nanowires. The band gap energies for 2.5 and 1.7 nm diameter nanowires can be estimated to be 3.47 and 3.69 eV, respectively. Comparing with the band gap (1.21 eV) of the bulk Cu₂S,⁴ there is obviously a large blue shift between them, indicating a stronger quantum size effect than that of the previously reported Cu₂S nanoparticles.^{6a} The high band gap of the product makes it a promising candidate for photovoltaic materials.

Conclusion

In summary, we have demonstrated a facile and effective solution-phase approach for the synthesis of high aspect ratio and ultrathin nanowires of hexagonal-phase Cu₂S with a diameter of less than 2.5 nm. The growth of Cu₂S nanowires was believed to be attributed to the synergistic effect of the solvent OA and the adsorbent affinities of DT. Such a solution-phase route using the mixed surfactants as the solvent may represent a promising way for the synthesis of high aspect ratio and ultrathin inorganic nanowires. In addition, by carefully adjusting the synthetic parameters, the resultant Cu₂S nanostructures could be selectively controlled to be nanowires, nanorods, and nanoparticles with various dimensions. Thus, this method also provides an efficient way for the synthesis of Cu₂S nanostructures with controllable shapes and sizes. Furthermore, a strong quantum size effect of the ultrathin nanowires that was revealed by UV-vis absorption spectrum suggests its promising application for photoelectric conversion.

Acknowledgment. This work was supported by the National Natural Science Foundation of China and the 973 Project of China.

References and Notes

- (1) (a) Alivisatos, A. P. *Science* **1996**, 271, 933. (b) Hu, J.; Odom, T. W.; Lieber, C. M. *Acc. Chem. Res.* **1999**, 32, 435. (c) Li, M.; Schnablegger, H.; Mann, S. *Nature* **1999**, 402, 393. (d) Peng, X.; Manna, L.; Yang, W.; Wickham, J.; Scher, E.; Kadavanich, A.; Alivisatos, A. P. *Nature* **2000**, 404, 59.
- (2) (a) Coombs, N.; Khushalani, D.; Oliver, S.; Ozin, G. A.; Shen, G. C.; Sokolov, I.; Yang, H. *J. Chem. Soc., Dalton Trans.* **1997**, 3941. (b) Bando, Y.; Takayanagi, K. *Science* **2000**, 289, 606. (c) Hong, B. H.; Bae, S. C.; Lee, C. W.; Jeong, S.; Kim, K. S. *Science* **2001**, 294, 348. (d) Holmes, J. D.; Johnston, K. P.; Doty, R. C.; Korgel, B. A. *Science* **2000**, 287, 1471. (e) Urban, J. J.; Yun, W. S.; Gu, Q.; Park, H. *J. Am. Chem. Soc.* **2002**, 124, 1186. (f) Shi, H.; Qi, L.; Ma, J.; Cheng, H. *Chem. Commun.* **2002**, 1704.
- (3) For example: (a) Jun, Y. W.; Lee, S. M.; Kang, N. J.; Cheon, J. J. *Am. Chem. Soc.* **2001**, 123, 5151. (b) Jun, Y. W.; Jung, Y. Y.; Cheon, J. J. *Am. Chem. Soc.* **2002**, 124, 615. (c) Dumestre, F.; Chaudret, B.; Amiens, C.; Fromen, M.; Casanove, M.; Renaud, P.; Zurcher, P. *Angew. Chem., Int. Ed.* **2002**, 41, 4289. (d) Dumestre, F.; Chaudret, B.; Amiens, C.; Respaud, M.; Fejes, P.; Renaud, P.; Zurcher, P. *Angew. Chem., Int. Ed.* **2003**, 42, 5213. (e) Qian, C.; Kim, F.; Ma, L.; Tsui, F.; Yang, P. D.; Liu, J. *J. Am. Chem. Soc.* **2004**, 126, 1195. (f) Grebinski, J. W.; Hull, K. L.; Zhang, J.; Kosel, T. H.; Kuno, M. *Chem. Mater.* **2004**, 16, 5260.
- (4) (a) Marshall, R.; Mitra, S. S. *J. Appl. Phys.* **1965**, 36, 3882. (b) *Numerical Data and Functional Relationships in Science and Technology—Physics of Non-Tetrahedrally Bonded Elements and Binary Compounds I*; Madelung, O., Ed.; Springer: Berlin, 1983; Vol. 17e, pp 137–153.
- (5) *Current Topics in Photovoltaics*; Coutts, T. J., Meakin, J. D., Eds.; Academic Press: Orlando, FL, 1985.
- (6) (a) Haram, S. K.; Mahadeshwar, A.; Dixit, S. G. *J. Phys. Chem.* **1996**, 100, 5868. (b) Zhang, P.; Gao, L. *J. Mater. Chem.* **2003**, 13, 2007.
- (7) Lu, Q.; Gao, F.; Zhao, D. *Nano Lett.* **2002**, 2, 725.

- (8) (a) Wang, S. H.; Yang, S. H. *Chem. Phys. Lett.* **2000**, 322, 567. (b) Wang, S. H.; Yang, S. H.; Dai, Z. R.; Wang, Z. L. *Phys. Chem. Chem. Phys.* **2001**, 3, 3750. (c) Wang, S. H.; Guo, L.; Wen, X. G.; Yang, S. H.; Zhao, J.; Liu, J.; Wu, Z. H. *Mater. Chem. Phys.* **2002**, 75, 32–38.
- (9) (a) Larsen, T. H.; Sigman, M.; Ghezelbash, A.; Doty, R. C.; Korgel, B. A. *J. Am. Chem. Soc.* **2003**, 125, 5638. (b) Sigman, M. B., Jr.; Ghezelbash, A.; Hanrath, T.; Saunders, A. E.; Lee, F.; Korgel, B. A. *J. Am. Chem. Soc.* **2003**, 125, 16050.
- (10) Chen, L.; Chen, Y. B.; Wu, L. M. *J. Am. Chem. Soc.* **2004**, 126, 16334.
- (11) Liu, Z. P.; Liang, J. B.; Xu, D.; Lu, J.; Qian, Y. T. *Chem. Commun.* **2004**, 2724.
- (12) Buerger, M. J.; Wuensch, B. J. *Science* **1963**, 141, 276.
- (13) Pike, R. D.; Cui, H.; Kershaw, R.; Wight, K. D.; Wold, A.; Blanton, T. N.; Wernberg, A. A.; Gysling, J. J. *Thin Solid Films* **1993**, 224, 231.
- (14) Lou, Y. B.; Samia, A. C. S.; Cowen, J.; Banger, K.; Chen, X. B.; Lee, H.; Burda, C. *Phys. Chem. Chem. Phys.* **2003**, 5, 1091.
- (15) For example: (a) Murry, C. B.; Norris, D. J.; Bawendi, M. G. *J. Am. Chem. Soc.* **1993**, 115, 8706. (b) Peng, X.; Schlamp, M. C.; Kadavanich, A.; Alivisatos, A. P. *J. Am. Chem. Soc.* **1997**, 119, 7019. (c) Peng, Z. A.; Peng, X. *J. Am. Chem. Soc.* **2001**, 123, 1389. (d) Joo, J.; Na, H. B.; Yu, T.; Yu, J. H.; Kim, Y. W.; Wu, F.; Zhang, J. Z.; Hyeon, T. *J. Am. Chem. Soc.* **2003**, 125, 11100.